Solid State Communications 151 (2011) 87–92

Contents lists available at ScienceDirect

Solid State Communications

journal homepage: www.elsevier.com/locate/ssc

Influence of phonon-associated tunneling rate on transport through a single-molecule transistor

Ying-Tsan Tang [a,*], Der-San Chuu [a], Kao-Chin Lin [b,**]

[a] Department of Electrophysics, National Chiao Tung University, Hsinchu 30013, Taiwan

[b] Department of Physics, National Cheng Kung University, Tainan 70101, Taiwan

ARTICLE INFO

Article history:
Received 2 July 2010
Received in revised form
21 September 2010
Accepted 5 October 2010
by S. Tarucha
Available online 14 October 2010

Keywords:
C. Phonon-assisted tunneling
C. Electron–phonon interactions
C. Electronic transport

ABSTRACT

We study the electronic transport through a single-molecule transistor (SMT) by considering the phonon-associated tunneling rate. We find that the electron–phonon interaction (EPI) changes the constant conductivities of the leads into a multi-channel structure of single vibration frequency. This interference of the multi-channel tunneling process results in a bias-dependent tunneling rate and obscures the conductance peaks at large bias voltage. The bias-dependent tunneling rate further causes a remarkable conductivity gap between the chemical potential of the leads ($n = 0$) and the first phonon sideband ($n = 1$). These anomalies are consistent with the experimental observations in transport experiments.

0. Introduction

Among the research topics of molecular devices, one of the particular interests in transport issues is to study charge states coupling to their vibrational or configurational modes. In recent years, as the trend of miniaturization of electronic devices continues, the influence of electron–phonon interaction (EPI) on a single-molecule transistor (SMT) system [1–4], as well as on a semiconductor quantum dot (QD) system [5,6], has received much attention and has been investigated experimentally by a number of groups. Some of them reported that single-molecule transistors could be strongly affected by a single-vibration mode. In Ref. [1], Park et al. showed that this kind of mechanical device can be realized by attaching a C_{60} molecule to the gold surface, where the single phonon mode of the C_{60} was induced via the van der Waals force and electrostatic interactions. They observed the staircase current and found oscillations of conductance as the bias in both terminals was increased. Later, Weig et al. successfully reproduced a similar staircase current by embedding a quantum dot on a freestanding GaAs/AlGaAs membrane [6], where a single-vibration mode is applied by an electron–phonon cavity. In a recent work published in Ref. [7], Leturcq et al. took advantage of a suspended carbon nanotube (CNT) to create a vibrating quantum dot for the observation of strong electron–phonon coupling effects on the current. They confirmed the phonon-blockade behavior at low-bias and probed conductance peaks in the Coulomb Blockade regions, where the phonon frequency is decided by the longitudinal phonons in the CNT.

The rate equation (RE) [8], the master equation [9–11] and the NEGF [12,13] have successfully explained many transport experiments. Each of these theoretical approaches has its own advantages and limitations. For instance, the RE rapidly yields the equation of motion for every state by directly replacing the density $\rho(t')$ by $\rho(t)$, that is, it can only work under a weak-coupling environment. In the report by Brandes [9], they calculated the main current of double quantum dots via the RE and concluded that the non-linear electric current stemmed from the shake-up effects of the phonons. Theoretically, the EPI induces phonon sidebands (PSB) in the spectral function and leads to satellite conductance peaks of PSB in mesoscopic nanostructures. These multiple peaks appear asymmetrically with respect to the renormalized level of the quantum dot, and a PSB can be acquired as the applied bias (eV_b) exceeds the required energy of the phonons [14–16]. To our knowledge, the non-equilibrium Green's function (NEGF) is a convincing tool for solving kinetic equations, particularly when the system is under non-equilibrium conditions [17,18] ($V_b \neq 0$). The advantage is that a state is well-defined in the far past and the historical evolution of the state is maintained well by the S-matrix. Basically, the evolution of the propagator in the NEGF is managed on a complex contour, not a real-time one.

* Corresponding author. Tel.: +886 3 5712121 56142; fax: +886 3 5728161.
** Corresponding author. Tel.: +886 6 2757575 65245.
E-mail addresses: yingtsan.tang@gmail.com (Y.-T. Tang), kaochin.lin@gmail.com (K.-C. Lin).

0038-1098/$ – see front matter © 2010 Elsevier Ltd. All rights reserved.
doi:10.1016/j.ssc.2010.10.007

In order to change the complex contour into real-time physical quantities, sophisticated mathematical techniques are required, and a transformation procedure called the analytic continuation, or the Langreth theorem (LT), is applicable [19]. In Ref. [17], one of the famous applications of the Langreth theorem on quantum transport was developed by Jauho, Wingreen, and Meir (JWM). In the conventional JWM's current formula [12], the entire system is divided into the leads and the central region, and the current can be obtained as we solve the Green's functions $G^{r,<}(\omega)$. Note that the JWM's formula possesses the self-consistent feature to fulfill the continuity rule [17]. Here, the self-consistency means that the bandwidth of the spectral function must coincide with the tunneling rate as solved by the Fermi golden rule.

In this paper the EPI system is studied under a small polaron-transformed frame [18], where the electron tunneling through the barrier is accompanied by a creation/annihilation of a phonon field [14,20,21], i.e. $V_{k\alpha}^{(*)} \rightarrow V_{k\alpha}X^{+}(X)$. According to the Fermi golden rule [18], the EPI may yield a phonon correlation involved in particle tunneling. So far most theoretical studies have attempted to separate the phonon correlation function from the interacting system via the Born approximation [12,14,18], i.e., the (EPI) retarded Green's function is written as a product of a (retarded) electron Green's function and a phonon correlation function. Even though this approach was proved to be successful in predicting the energy for emission (or absorption) of a phonon, it may cause phonon sidebands, which disagrees with experiments in the zero-phonon resonant tunneling regime [14]. In practice, this is because some correlations were not taken into consideration in the calculations referred to in Table 4.1 of Ref. [17]. In order to correct this conflicting sideband, Chen et al. [22] utilized the current formula derived by Wingreen and Meir [13] and studied from the lesser/greater Green's function. Consequently, a generalized current formula was obtained, and was able to work at zero bias voltage and arbitrary temperatures. Nonetheless, these theoretical predictions still do not coincide with the experimental results. For example, at $e|V_b| > \omega_0$, there exists a conductivity gap between the sidebands of $n = 0$ and $n = 1$ in experiments [1], while it is absent through the mean-field theory (MFT) calculations, which is due to the inappropriate treatment of the electron Green's function in the dot system. Note that in Ref. [22], Chen and co-workers imposed a concept of an average field to simplify the particle transport through the EPI system (MFT). The mean-field implies that the particle interacts with only the average field of the others, i.e., the systems are at equilibrium, and hence the interaction field operator may be replaced by a scalar field $V_{k\alpha}X^{+}(X) \rightarrow V_{k\alpha}\langle X\rangle$. However, this scalar assumption is insufficient to describe the particle transport properties caused by the EPI effect, to be specific, when the bias voltage was turned on at some t_0, i.e., the system is now at non-equilibrium. Hence, the relevant time-dependent interactions, such as phonon quantities such as $\langle X(t)X^{+}(t')\rangle$ should be treated as the contour-ordered Green's function, and then the application of the Langreth rule gives the real time Green's functions. In this article, we ignore the higher-order tunneling process induced by the heating of vibration or mutual influence in sub-electronic and sub-phononic systems, and treat the lead electrons and the phonons as in equilibrium. That is, we focus on the lowest-order electron–phonon interaction. In addition, the spin degree of freedom and the influence of Coulomb interaction are also omitted.

1. Physical model and formulation

1.1. Model

The electron transport between the leads and the central region is considered as shown in Fig. 1. For example, in a single resonant QD or SMT, electrons vibrate at a single frequency ω_0. The EPI system is studied theoretically through a non-perturbative

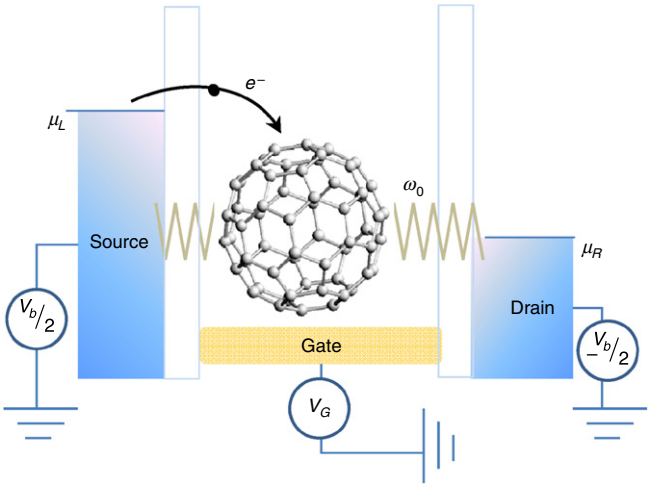

Fig. 1. A vibrating single-molecule transistor (C_{60}).

canonical transformation $\overline{H} = e^{S}He^{-S}$ with $S = (\lambda/\omega_0)\, d^{+}d\left(b^{+} - b\right)$ [14,18,22]. Under this unitary transformation, the Hamiltonian now reads:

$$\overline{H} = \overline{H}_{\text{cen}} + \overline{H}_{\text{lead}} + \overline{H}_{T},$$

$$\overline{H}_{\text{cen}} \equiv \bar{\varepsilon}_0\left(V_g\right) d^{+}d + \omega_0 b^{+}b, \tag{1}$$

$$\overline{H}_{\text{lead}} = \sum_{k_\alpha,\alpha\in L,R} \varepsilon_{k_\alpha} c_{k_\alpha}^{+} c_{k_\alpha}, \tag{2}$$

$$\overline{H}_{T} = \sum_{k_\alpha,\alpha\in L,R} V_{k_\alpha} c_{k_\alpha}^{+}\mathrm{d}X + h.c, \tag{3}$$

where

$$X \equiv \exp\left[-\frac{\lambda}{\omega_0}\left(b^{+} + b\right)\right]. \tag{4}$$

The operators $d^{+}(d)$ and $c_{k_\alpha}^{+}\left(c_{k_\alpha}\right)$ represent the creation (annihilation) operators of the electron in the QD (or SMT) and the α lead, respectively. The operator $b^{+}(b)$ is the creation (annihilation) operator of the phonon. $\bar{\varepsilon}_0 \equiv \varepsilon_0\left(V_g\right) - \Delta$ is the dot level energy controlled by the gate voltage, with the canonical energy shift $\Delta = \lambda^2/\omega_0$. The coupling strength of EPI is denoted by λ and the tunneling matrix element between the QD (or SMT) and the α lead is defined as V_{k_α}. Here ε_{k_α} is the energy of the electron in the α lead, which remains unchanged because of the absence of phonon field in the α lead.

1.2. The transport formula and self-energy

The current from the left lead to the central region can be defined [12] as

$$J_L(t) = \frac{2\mathrm{e}}{\hbar}\mathrm{Re}\sum_{k,\alpha\in L} V_{k\alpha,d}G_{d,k\alpha}^{<}\left(t,t'\right)|_{t'\rightarrow t} \tag{5}$$

where the Green's function $G_{d,k\alpha}^{<}\left(t,t'\right) \equiv \mathrm{i}\left\langle c_{k\alpha}^{+}\left(t'\right)X\left(t'\right)d(t)\right\rangle$ together with its conjugate property are applied above. Note that the interaction is mutual, both terminals are vibrating from the perspective of the quantum dot, hence $c_{k\alpha}^{+}$ and X evolve at the same time. Performing the continuation rules [12] on $G_{d,k\alpha}\left(\tau,\tau'\right)$ and substituting the resulting $G_{d,k\alpha}^{<}\left(t,t'\right)$ into Eq. (5), we obtain:

$$J_L(t) = -\frac{2\mathrm{e}}{\hbar}\mathrm{Im}\left[\int_{-\infty}^{t}\mathrm{d}t_1 G_{dd}^{r}\left(t,t_1\right)\Sigma_{\alpha\epsilon L}^{<}\left(t_1,t\right) + G_{dd}^{<}\left(t,t_1\right)\Sigma_{\alpha\epsilon L}^{a}\left(t_1,t\right)\right], \tag{6}$$

where the partial part of the tunneling self-energy can be found as

$$\Sigma_{\alpha}^{a}\left(t,t'\right)=-\theta\left(-t+t'\right)\sum_{n}\left[\Sigma_{\alpha,n}^{>}\left(t,t'\right)-\Sigma_{\alpha,n}^{<}\left(t,t'\right)\right]. \tag{7}$$

Here $\Sigma_{\alpha,n}^{>,<}=F^{+>,<}\cdot\sum_{k_\alpha}|V_{k\alpha}|^2\,g_{k\alpha}^{>,<}$. $F^{+>}(t-t')\equiv\langle X^{+}(t')X(t)\rangle$ and $F^{+<}\left(t-t'\right)\equiv\left\langle X(t)X^{+}\left(t'\right)\right\rangle$ are the greater and lesser phonon Green's functions, and $g_{k\alpha}^{<(>)}\left(t-t'\right)$ is the lesser (greater) Green's function for the free electron in the α lead. The Fourier transform of the self-energies in Eq. (7) leads to:

$$\begin{aligned}\Sigma_{\alpha,n}^{r,a}(\omega)&=\sum_{k\alpha}\left[p_n\frac{V_{k\alpha}^{*}V_{k\alpha}}{\omega+n\omega_0-\varepsilon_{k\alpha}\pm\mathrm{i}\delta}f_{\alpha}^{<}(\varepsilon_{k\alpha})\right.\\&\left.+p_{-n}\frac{V_{k\alpha}^{*}V_{k\alpha}}{\omega+n\omega_0-\varepsilon_{k\alpha}\pm\mathrm{i}\delta}f_{\alpha}^{>}(\varepsilon_{k})\right],\end{aligned} \tag{8}$$

$$\begin{aligned}\Sigma_{\alpha,n}^{\gtrless}(\omega)&=\sum_{k\alpha}V_{k\alpha}^{*}V_{k\alpha}p_{\mp n}g_{k\alpha}^{\gtrless}(\omega+n\omega_0)\\&=\mp\mathrm{i}\sum_{n}p_{\mp n}\Gamma_{\alpha}(\omega+n\omega_0)f_{\alpha}^{\gtrless}(\omega+n\omega_0),\end{aligned} \tag{9}$$

where $f_{\alpha}^{<}(\varepsilon_{k\alpha})$ and $f_{\alpha}^{>}(\varepsilon_{k\alpha})$ are the electron and hole Fermi functions in the α lead. In this paper, $\Gamma_{\alpha}(\omega)=2\pi\sum_{k\alpha}|V_{k\alpha}|^2\,\delta(\omega-\varepsilon_{k\alpha})$ represents the rate of a particle leaving the quantum dot system without the EPI. The factor p_n denotes the weighting function of the interactions between the electron and n phonons, which is found as $p_n=\mathrm{e}^{-2g\left(N_0+\frac{1}{2}\right)}\mathrm{e}^{n\omega_0/2k_BT}I_n\left(2g\sqrt{N_0(N_0+1)}\right)$ [18], where N_0 and I_n are the Bose function and the modified Bessel function.

1.3. The spectral function

In frequency space, the appliance of the LT on the self-consistent Dyson equation of the electron Green's function in the QD (or SMT) [17,18] leads to $G_{dd}^{r,a}(\omega)=\left[\omega-\bar{\varepsilon}_0-\Sigma_T^{r,a}(\omega)\right]^{-1}$, where the contour-ordered self-energy Σ_T induced by the tunneling process reads $\Sigma_T(\omega)=F^{+}(\omega)\,\widetilde{\Sigma}_T(\omega)$, and it carries the information on the lead electrons and phonons. From the definition of the spectral function $A_d(\omega)=-2\mathrm{Im}\,G_{dd}^{r}(\omega)$, we get:

$$A_d(\omega)=\frac{\sum_{n,\alpha}\left[p_n\Gamma_{\alpha}f_{\alpha}^{<}(\omega+n\omega_0)+p_{-n}\Gamma_{\alpha}f_{\alpha}^{>}(\omega+n\omega_0)\right]}{\left(\omega-\widetilde{\varepsilon}_0\right)^2+\left[W(\omega)/2\right]^2}, \tag{10}$$

where $\widetilde{\varepsilon}_0=\bar{\varepsilon}_0\left(V_g\right)-\mathrm{Re}\,\Sigma_T^{r}(\omega)$ denotes the renormalized level position, and $W(\omega)=-2\mathrm{Im}\Sigma_T^{r}(\omega)$ represents the life-time broadening (bandwidth) of the dot state. A comparison with the conventional JWM's formula in Ref. [17] assures that the life-time broadening of a dot state $W(\omega)$ in Eq. (10) equals the summation of out-tunneling rates between the leads and the system, i.e. Eq. (8); Eq. (6) is therefore self-consistent and meaningful. Note that $G_{dd}^{<}(\omega)$ in Eq. (6) can be quickly solved via using the Keldysh equation $G_{dd}^{<}=\left|G_{dd}^{r}\right|^2\Sigma_T^{<}(\omega)$ [12]. The remaining goal is to decide the retarded self-energy $\Sigma_T^{r}(\omega)$. To this end, $\sum_{k\alpha}$ is replaced by $\int\mathrm{d}\omega\rho(\omega)$, and the Lorentz density of states with bandwidth E_C at the chemical potential μ_α is assumed [20,21]. With this auxiliary function, the integral becomes convergent, and the retarded self-energy of the electron in QD (SMT) reads

$$\begin{aligned}\mathrm{Re}\,\Sigma_T^{r}(\omega)&=\sum_{n,\alpha}\left(p_n-p_{-n}\right)\frac{\Gamma_{\alpha}(\omega+n\omega_0)}{2\pi}\left[\ln\left(\frac{E_C}{2\pi k_BT}\right)\right.\\&\left.-\mathrm{Re}\psi\left(\frac{1}{2}+\mathrm{i}\frac{\omega+n\omega_0-\mu_\alpha}{2\pi k_BT}\right)\right],\end{aligned} \tag{11}$$

$$\begin{aligned}\mathrm{Im}\,\Sigma_T^{r}(\omega)&=\frac{1}{2\pi}\sum_{n,\alpha}\left[p_n\Gamma_{\alpha}(\omega+n\omega_0)f_{\alpha}^{<}(\omega+n\omega_0)\right.\\&\left.+p_{-n}\Gamma_{\alpha}(\omega+n\omega_0)f_{\alpha}^{>}(\omega+n\omega_0)\right].\end{aligned} \tag{12}$$

$\psi(z)$ is the digamma function with a complex argument. It can be seen from Eq. (11) that besides the energy shift Δ due to the canonical transformation, another energy shift $\mathrm{Re}\,\Sigma_T^{r}(\omega)$ is obtained from the phonon correlation function. In addition to the renormalization shift, we find that the life-time broadening of Eq. (12) from the LT is more complicated than that from the MFT [22], which is a constant. It is because the LT preserves the properties of electrons and holes in the leads via the phonon Green's functions.

1.4. The Landauer–Büttiker formula

The Landauer–Büttiker formula [23,24] can be used to describe the current from one lead to another, and may be derived through the Green's function [12]. Using the identical relations of $G^{r}-G^{a}=G^{>}-G^{<}$ and $\Sigma^{r}-\Sigma^{a}=\Sigma^{>}-\Sigma^{<}$ in Eq. (6), an alternative expression of current is acquired as:

$$\begin{aligned}J_\alpha=\frac{\mathrm{e}}{\hbar}\int\frac{\mathrm{d}\omega}{2\pi}\sum_{n,n'}\left[T_{nn'}^{\alpha\bar{\alpha}}(\omega)f_{\alpha}^{<}(\omega+n\omega_0)f_{\bar{\alpha}}^{>}\left(\omega-n'\omega_0\right)\right.\\\left.-T_{n'n}^{\bar{\alpha}\alpha}(\omega)f_{\alpha}^{>}(\omega-n\omega_0)f_{\bar{\alpha}}^{<}\left(\omega+n'\omega_0\right)\right],\end{aligned} \tag{13}$$

where the tunneling function $T_{nn'}^{\alpha\bar{\alpha}}$ is defined as

$$T_{nn'}^{\alpha\bar{\alpha}}(\omega)=p_np_{n'}\frac{\Gamma^{\alpha}(\omega+n\omega_0)\,\Gamma^{\bar{\alpha}}\left(\omega-n'\omega_0\right)}{W(\omega)}A_d(\omega). \tag{14}$$

Eqs. (13) and (14) are the central formulas for studying the joint effect due to the phonon-associated tunneling rate. Moreover, Eq. (13) provides a clearer picture of EPI transport than Eq. (6) does, that is, the electron departs from the n-th (electron) state in the α lead (source), tunnels through the dot, and arrives at the n'-th (hole) state in the $\bar{\alpha}$ lead (drain). In general, the electron states are located below the chemical potential and the hole states above. Fig. 2(a) shows a graphical illustration for this description for a low-lying level position $\bar{\varepsilon}_0=-\omega_0$ (left), medium level $\bar{\varepsilon}_0=0$ (central), and higher level $\bar{\varepsilon}_0=\omega_0$ (right), where the bias is at $eV_b=2\omega_0$, and the red arrows indicate the significant channels for particles passing through the dot. From Eq. (14), we see that $T_{nn'}^{\alpha\bar{\alpha}}$ is expressed in terms of the spectral function, tunneling rates, and weight factors on both terminals p_n and $p_{n'}$ due to the EPI effect. At zero temperature, the weight factor p_n is zero for $n<0$ [22], the Fermi function goes towards a step function, and the transport window for each channel, i.e. $\theta(\mu_\alpha-\omega-n\omega_0)\,\theta\left(\omega-n'\omega_0-\mu_{\bar{\alpha}}\right)$, in Eq. (13) is given by $\varepsilon_{\alpha,-n}^{F}-\varepsilon_{\bar{\alpha},n'}^{F}=\mu_\alpha-\mu_{\bar{\alpha}}-\left(n+n'\right)\omega_0$. At low temperature, the particle transport practices are within μ_L and μ_R. However, at high temperature, $p_{-\|n\|}$ is non-zero, and hence the phonon-mediated states outside the transport window also participate. Therefore, the current in this field is probable [7].

An analogous transport scheme has been presented in previous publications [11,12,14,16,22,25,27], although the background physics is different. For example, in Refs. [14] and [22] the n-th phonon-mediated state exists in the QD (or SMT) because the phonon field is treated as being involved in the evolution of the dot, so the phonon sidebands come from the SMT electrons and holes. Note that the quantized number is labeled from the energy of the dot, not from the chemical potential of the leads. Furthermore, Dong et al. [25] performed a mapping technique to reach a

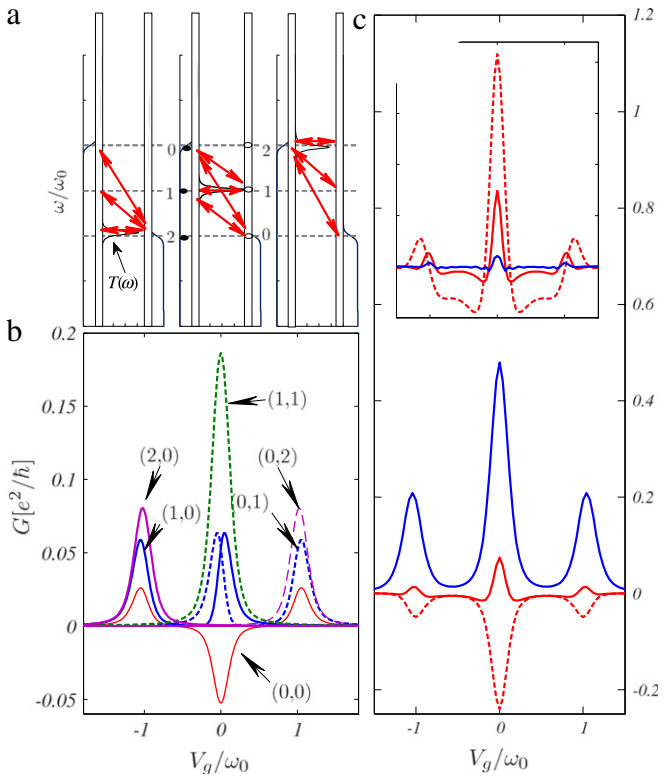

Fig. 2. (Color online) (a) A schematic description of the transport channels and tunneling coefficient at different gate voltages. Here • represents the electron state (labeled from the chemical potentail of the left lead μ_L) and ○ the hole state (from the chemical potential of the right lead μ_R). The red arrow denotes the transport path. (b) The differential conductance for each channel, where the quantum pair (n, n') means that the particle transports from the n-th phonon-mediated state in the α lead (electron state •) to the n'-th phonon-mediated state in the $\bar{\alpha}$ lead (hole state ○). The parameters of the system are $\Gamma_L = \Gamma_R = 0.2\omega_0$, $k_BT = 0.05\omega_0$, $\lambda = 1.5\omega_0$, $\mu_L = -\mu_R = \omega_0$ and the Lorentz cut-off is $E_C = 100$ in the integral calculation [21]. (c) Differential conductance in the leads G_{lead} (blue line) and in the dot $G^{s,l}_{\text{lead}}$ (red lines), where G^s_{dot} (solid line) is induced by the EPI renormalization, and G^l_{dot} (dotted line) is caused by the level broadening. The inset shows that the conductance G^s_{dot} becomes significant at strong electron–electron coupling (red dotted line, $\Gamma_L = \Gamma_R = 0.6\omega_0$) while it is highly supressed at strong electron–phonon coupling (blue line, $\lambda = 2\omega_0$).

Landauer–Büttiker formula similar to the one in Eq. (13). However, since the phonon correlation is not involved in the tunneling self-energy, this technique results in a bias-independent bandwidth in the tunneling function, no matter what approximation is adopted. It is worth mentioning that the results obtained by Braig and Flensberg [27] through the RE are similar to those of ours, and a comparison is made in Section 2.2.

1.5. Differential conductance

Taking the derivative of Eq. (13) with respect to the bias voltage, the differential conductances can be expressed as:

$$G = G_{\text{lead}} + G_{\text{dot}}, \tag{15}$$

$$G_{\text{lead}} = \frac{e}{\hbar}\int \frac{d\omega}{2\pi}\sum_{n,n'} T^{\alpha\bar{\alpha}}_{nn'}(\omega) f'_{nn'}(\omega), \tag{16}$$

$$G_{\text{dot}} = \frac{e}{\hbar}\int \frac{d\omega}{2\pi}\sum_{n,n'} \frac{\partial T^{\alpha\bar{\alpha}}_{nn'}(\omega)}{\partial V_b} f_{nn'}(\omega), \tag{17}$$

$$f_{nn'}(\omega) = f^<_\alpha(\omega + n\omega_0) f^>_{\bar{\alpha}}(\omega - n'\omega_0) - f^<_{\bar{\alpha}}(\omega + n\omega_0) f^>_\alpha(\omega - n'\omega_0), \tag{18}$$

where the wide-band limit is considered, and G_{lead} and G_{dot} are defined as the conductance in the leads and in the QD (or SMT) system, respectively. $J_\alpha(\omega)$ is the current density, $f_{nn'}(\omega)$ determines the effective transport window and the derivative of the Fermi function with respect to the bias reflects a thermal broadening function in the leads [26],

$$f'_{nn'}(\omega) = \beta\sum_{\eta\in\pm1}\left\{\frac{f^>_R(\eta\omega - n'\omega_0)}{8\cosh^2\left[\frac{\beta}{2}(\omega + \eta n\omega_0 - \mu_L)\right]} + \frac{f^<_L(\eta\omega - n\omega_0)}{8\cosh^2\left[\frac{\beta}{2}(\omega - \eta n'\omega_0 - \mu_R)\right]}\right\}. \tag{19}$$

For $eV_b > 0$, $f'_{nn'}(\omega)$ shows multiple peaks at $\omega = \varepsilon^F_{\alpha,-n}(= \mu_\alpha - n\omega_0)$ and $\omega = \varepsilon^F_{\bar{\alpha},n}(= \mu_{\bar{\alpha}} + n\omega_0)$, where n and $n' = 0, 1, 2$ and so on. Substituting Eq. (19) back into Eq. (16), it is found that G_{lead} reaches its maximum when the dot level matches the thermal broadening peaks. Therefore, when drawing G_{lead} versus V_g (see Fig. 2(c)), the satellite peaks of differential conductance are at $V_g = \varepsilon^F_{\alpha,-n}$ and $\varepsilon^F_{\bar{\alpha},n}$, symmetrically distributed with respect to $V_g = 0$.

2. Results and discussion

The interference of the multi-channel tunneling process plays an important role in the quantum transport. This effect may shift the level position to higher energies and cause the bias-dependent bandwidth of the tunneling function in the interacting system, and further leads to the conductivity gap between the chemical potential of the leads ($n = 0$) and the first phonon sideband ($n = 1$).

2.1. The influence of the EPI energy shift

According to Eq. (17), the conductivity probed in the dot can be further divided into two parts,

$$G^{s(l)}_{\text{dot}} = \frac{e}{\hbar}\int \frac{d\omega}{2\pi} J_\alpha(\omega) K_{s(l)}(\omega), \tag{20}$$

where G^s_{dot} and G^l_{dot} respectively characterize the conductance induced by the energy shift and the bandwidth of the dot level, and $K_s(\omega)$ and $K_l(\omega)$ are solved as

$$K_s(\omega) = -\left\{\begin{array}{l}\text{Re}G^r(\omega)\cdot\left[\sum_{n,\alpha\in L,R}(p_n - p_{-n})\Gamma^\alpha(-1)^{\delta_{L,\alpha}}\right] \\ \beta\text{Im}\psi_1\left(\frac{1}{2} + i\frac{\beta}{2\pi}(\omega + n\omega_0 - \mu_\alpha)\right)\end{array}\right\}, \tag{21}$$

$$K_l(\omega) = A_d(\omega) W'(\omega), \tag{22}$$

$$W'(\omega) = \beta\sum_{n,\alpha\in L,R}\frac{(p_n - p_{-n})\Gamma^\alpha(-1)^{\delta_{L,\alpha}}}{16\cosh^2\left[\frac{\beta}{2}(\omega + n\omega_0 - \mu_\alpha)\right]}.$$

A comparison between G^s_{dot} and G^l_{dot} in Fig. 2(c) gives that G^l_{dot} is always negative while G^s_{dot} is positive at the quantized levels of phonon-mediated states $(eV_g = n\omega_0)$. In addition, G^s_{dot} also exhibits a logarithmic energy dependence near the quantized level, as depicted in the inset of Fig. 2(c). In practice, this is due to the consideration of the EPI-renormalized energy shift during particle transport. A comparison of G^s_{dot} in the inset of Fig. 2(c) shows that the energy-shift dependence becomes more apparent (dotted line) as the electron–electron coupling is increased ($\Gamma_L = \Gamma_R = 0.6\omega_0$), whereas it is highly suppressed when increasing the intensity of the EPI. This is because of the existence of e^{-g} in the weighting factor p_n.

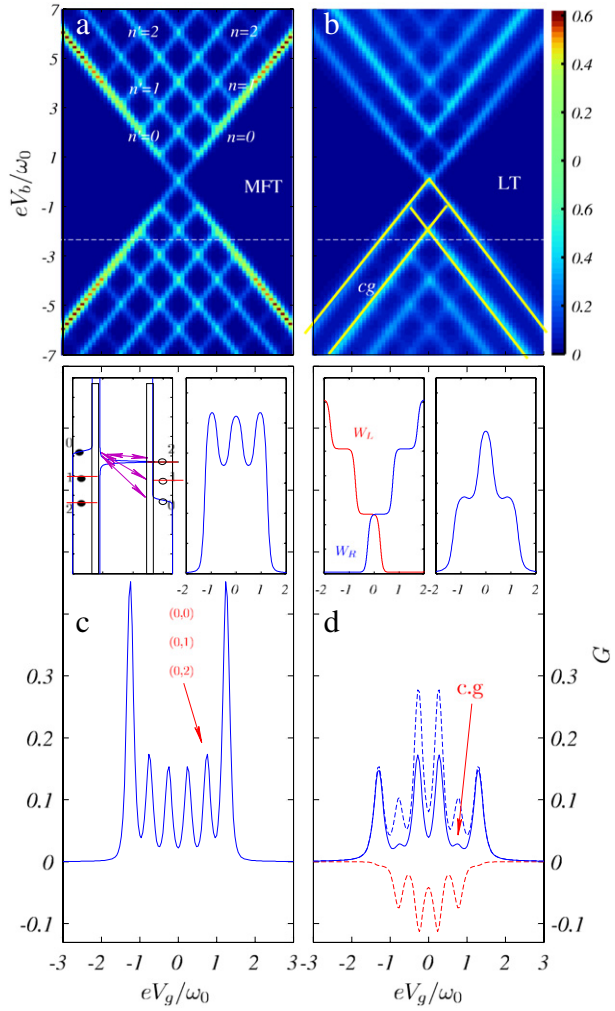

Fig. 3. (Color online) The conductance map versus the gate voltage V_g and the bias voltage V_b, where (a) is solved with the MFT method and (b) with the LT method. In (b), a gap always exists between the edge of the conductance (chemical potential, $n = 0$) and the first phonon-mediated state ($n = 1$). Note that the parameters are the same in Figs. 2 and 3. The differential conductance as a function of the gate voltage is plotted at $eV_b = 2.5\omega_0$. Left inset: the schematic description of particle transport through the dot at $eV_g = 0.75\omega_0$. There exist three channels for particle transport, $(0, 0)$, $(0, 1)$, and $(0, 2)$. Right inset: the MFT-PAT current. (d) The conductance in the leads (blue dashed line) and in the dot (red dashed line). The solid line is the total conductance, and the arrow indicates the occurrence of the conductivity gap. Left inset: the phonon-associated tunneling rate due to the left and the right leads (W_L and W_R). Right inset: the LT-PAT current, where no resonant peak occurs at $eV_g = 0.75\omega_0$.

2.2. Conductivity gap

Next we investigate an experimentally observable feature induced by the phonon-associated tunneling rate, the conductance gap [1] (cg). Comparison of Fig. 3(a) and (b) suggests that a gap always exists between the edge of the conductance (chemical potential, $n = 0$) and the first phonon-mediated state ($n = 1$); however, no conductance gap appears in the MFT calculation. In the MFT, the current can be understood as an effective particle propagating in an average field between the multi-channel leads, where the spectral function of the dressed electron in the dot is given by $A_d(\omega) = \widetilde{\Gamma}/[(\omega-\overline{\varepsilon}_0)^2 + \widetilde{\Gamma}^2]$ with $\widetilde{\Gamma} = (\Gamma_L+\Gamma_R)\langle X\rangle^2/2$, which is independent of the bias, analogous to the model without EPI. Taking $A_d(\omega)$ in Eqs. (15)–(18), we obtain $G = G_{\text{lead}}$, and hence the conductance peak represents the vacant phonon-mediated states in the wire. In general, the bandwidth is the decay rate, i.e., the out-tunneling rate. At dynamic equilibrium, the total out-tunneling rate is supposed to balance the sum of the in-tunneling rates so as to satisfy the continuity rule. Nevertheless, in the MFT the in-tunneling rate is bias-related while the out-tunneling rate is a constant, which signifies that some information, such as electrical properties, will be lost during the transport.

According to the derivations in Eq. (6), we obtain $W(\omega) = -2\text{Im}\,\Sigma_T^r(\omega)$ from the LT method, meaning that the level broadening of the dot equals the summation of out-tunneling rates between the leads and the system. From Eq. (12), we find that the electric information of the leads is kept via the electron–phonon correlation function. Since the Fermi functions are non-uniformly enhanced by the phonons (weighting factors), G_{dot} has a great impact when W is differentiated with respect to the bias.

Fig. 3(d) gives the profile of G_{lead} and G_{dot} versus eV_g at $eV_b = 2.5\omega_0$. We can see that G_{dot} presents a similar peak-structure to G_{lead}, but with negative amplitude. In order to analyze those peaks, we can perform the weak-coupling limit [17]. The weak coupling, that is, the spectral function in Eq. (10) taking the form of $A_d(\omega) = 2\pi\delta(\omega-\overline{\varepsilon}_0)$, is performed on Eqs. (16), (17) and (13), which gives

$$G_{\text{lead}} = \frac{e}{\hbar}\frac{\Gamma^\alpha\Gamma^{\overline{\alpha}}}{W(\overline{\varepsilon}_0)}\sum_{n,n'} p_n p_{n'} f'_{nn'}(\overline{\varepsilon}_0), \tag{23}$$

$$G^{(l)}_{\text{dot}} = -\frac{e}{\hbar}J(\overline{\varepsilon}_0)\,W'(\overline{\varepsilon}_0), \tag{24}$$

$$J(\overline{\varepsilon}_0) = \frac{e}{\hbar}\frac{\Gamma^\alpha\Gamma^{\overline{\alpha}}}{W(\overline{\varepsilon}_0)}\sum_{n,n'} p_n p_{n'} f_{nn'}(\overline{\varepsilon}_0). \tag{25}$$

G^s_{dot} does not exist since $\text{Re}\,\Sigma_T^r(\omega)$ approaches zero at small Γ. This is a good approximation because Eqs. (23)–(25) satisfy the definition of $G = \partial J(\overline{\varepsilon}_0)/\partial V_b$. Moreover, when rewriting $p_{-n} = p_n e^{-\beta n\omega_0}$ in $W(\overline{\varepsilon}_0)$ and $f_{nn'}(\overline{\varepsilon}_0)$, and performing some algebra, we readily reach the same current expression for a single resonant model as reported by Braig and Flensberg [27]. This is because the application of the RE, a method used to describe the quantum transport as the correlations in the system are much shorter than the electron transfer time, is equivalent to the expression of $A_d(\omega) = 2\pi\delta(\omega-\overline{\varepsilon}_0)$ in the NEGF [28,29].

Next, we consider the source of the conductance gap. At zero temperature, the summation of Eqs. (23) and (24) leads to:

$$\begin{aligned} G &= G_{\text{dot}} + G_{\text{lead}} \\ &= \frac{e}{\hbar}\frac{\Gamma^L\Gamma^R e^{-2g}}{W^2_{T=0}(\overline{\varepsilon}_0)}\sum_{n,n'}\frac{g^{n+n'}}{n!n'!}\Big[W'_{T=0}(\overline{\varepsilon}_0)\,f_{nn'}(\overline{\varepsilon}_0) \\ &\quad + W_{T=0}(\overline{\varepsilon}_0)\,f'_{nn'}(\overline{\varepsilon}_0)\Big], \end{aligned} \tag{26}$$

where $W_{T=0}$ and $f_{nn'}$ consist of multiple step functions, and $W'_{T=0}(\overline{\varepsilon}_0)$ and $f'_{nn'}(\overline{\varepsilon}_0)$ comprise delta functions. In the MFT, $W_{T=0}(\overline{\varepsilon}_0) = \widetilde{\Gamma}$, which is a constant such that $W'_{T=0}(\overline{\varepsilon}_0) = 0$ and $G = G_{\text{lead}}$. Consequently, Eq. (26) is directly proportional to the thermal broadening function $f'_{nn'}(\overline{\varepsilon}_0)$, and results in a multiple peak structure, as depicted in Fig. 3(c). At $eV_g/\omega_0 = 0.75$, three available channels $(0, 0)$, $(0, 1)$, and $(0, 2)$ contribute to the tunneling current (see the left inset of Fig. 3(c)). However, for the LT method, $W'_{T=0}(\overline{\varepsilon}_0)$ is non-zero at $eV_g/\omega_0 = 0.75$. Taking these quantum pairs in Eq. (26) reveals that G_{dot} and G_{lead} are of the same order and cancel each other out (see Fig. 3(d)), suggesting that the existence of a phonon-associated tunneling rate would greatly scale down the current and lead to a conductance gap in this field. The current–voltage characteristics in the right inset of Fig. 3(d) reflect this phenomenon. From the viewpoint of physics, this means that a virtual state is generated in this energy field. It is the first time that such a conductivity gap has been examined theoretically in the quantum dot system.

3. Conclusion

By applying the small polaron transformation and non-equilibrium Green's function (NEGF) technique, we examine the joint effects due to the phonon-associated tunneling rate. We suggest a useful transport formula and derive its corresponding spectral function to satisfy the continuity rule of the conventional JWM's formula. We find that, as the phonons are coupled to the electron tunneling process, the relevant phonon correlation breaks the electron–hole symmetry in the non-interacting terminals, making the tunneling rate change as a quantized feature of the vibration frequency. With the help of the Landauer–Büttiker formula, we recognize that the complex phonon-assisted tunneling process could be remodeled into a single-level quantum dot coupling to multi-channel leads. The current is written as a sum of all tunneling flux via different channels. The conventional effective single-particle transportation based on the mean-field theory is shown to be insufficient to interpret the phonon-assisted tunneling process. We find that the channel interference effect obscures the conductance map as the bias is increased. Such interference effects also lead to a significant conductance gap between the chemical potential of the leads and the first phonon-mediated state. This behavior has been widely observed in experiments but not explored theoretically before.

We hope that this new transport scheme together with the study of the phonon-associated tunneling rate will provide useful insights into the quantum transport field, and that more new physics like the low-frequency noise will be progressively explored in the future.

Acknowledgements

Finally, the authors would like to acknowledge valuable discussion with Prof. M. F. Lin, the team leader of the graphene group in the Department of Physics at NCKU, and Dr. Carlo Pagano at Institute of High Frequency and Semiconductor System Technologies in TU Berlin, and we are thankful for the support of the NSC-DAAD Sandwich Program under the grant number 96-2911-I-009-025-2 and the National Science Council, Taiwan under the grant number NSC 97-2112-M-009 -004, NSC 97-2112-M-110-001-MY2.

References

[1] H. Park, J. Park, A.K.L. Lim, E.H. Anderson, A.P. Alivisatos, P.L. McEuen, Nature 407 (2000) 57.
[2] L.H. Yu, D. Natelson, Nano Lett. 4 (2004) 79.
[3] S. Sapmaz, P. Jarillo-Herrero, J. Kong, C. Dekker, L.P. Kouwenhoven, H.S.J. van der Zant, Phys. Rev. B 71 (2005) 153402.
[4] S. Sapmaz, P. Jarillo-Herrero, Y.M. Blanter, C. Dekker, H.S.J. van der Zant, Phys. Rev. Lett. 96 (2006) 026801.
[5] R. Leturcq, C. Stampfer, K. Inderbitzin, L. Durrer, C. Hierold, E. Mariani, M.G. Schultz, F. von Oppen, K. Ensslin, Nat. Phys. 5 (2009) 327–331.
[6] E.M. Weig, R.H. Blick, T. Brandes, J. Kirschbaum, W. Wegscheider, M. Bichler, J.P. Kotthaus, Phys. Rev. Lett. 92 (2004) 046804.
[7] R. Leturcq, C. Stampfer, K. Inderbitzin, L. Durrer, C. Hierold, E. Mariani, M.G. Schultz, F. von Oppen, K. Ensslin, Nat. Phys. 5 (2009) 327–331.
[8] S.A. Gurvitz, Ya.S. Prager, Phys. Rev. B 53 (1996) 15932–15943.
[9] T. Brandes, B. Kramer, Phys. Rev. Lett. 83 (1999) 3021–3024.
[10] R. Aguado, T. Brandes, Phys. Rev. Lett. 92 (2004) 206601.
[11] A. Mitra, I. Aleiner, A.J. Millis, Phys. Rev. B 69 (2004) 245302.
[12] A.P. Jauho, N.S. Wingreen, Y. Meir, Phys. Rev. B 50 (1994) 5528.
[13] Y. Meir, N.S. Wingreen, Phys. Rev. Lett. 68 (1992) 2512.
[14] J.-X. Zhu, A.V. Balatsky, Phys. Rev. B 67 (2003) 165326.
[15] M. Galperin, A. Nitzan, M.A. Ratner, Phys. Rev. B 73 (2006) 045314.
[16] A. Zazunov, D. Feinberg, T. Martin, Phys. Rev. B 73 (2006) 115405; A. Zazunov, T. Martin, Phys. Rev. B 76 (2007) 033417.
[17] H. Haug, A.P. Jauho, Quantum Kinetics in Transport and Optics of Semiconductors, second ed., Springer, 2007.
[18] G.D. Mahan, Many Particle Physics, Plenum, New York, 1981, (Section 5.5B).
[19] D.C. Langreth, P. Nordlander, Phys. Rev. B 43 (1991) 2541–2557.
[20] J. König, J. Schmid, H. Schoeller, G. Schön, Phys. Rev. B 54 (1996) 16820.
[21] J. König, H. Schoeller, G. Schön, Phys. Rev. Lett. 76 (1996) 1715–1718.
[22] Z.Z. Chen, R. Lu, B.F. Zhu, Phys. Rev. B 71 (2005) 165324.
[23] R. Landauer, Phil. Mag. 21 (1970) 863.
[24] M. Büttiker, Phys. Rev. Lett. 57 (1986) 1761.
[25] B. Dong, H.L. Cui, X.L. Lei, Phys. Rev. B 69 (2004) 205315.
[26] S. Datta, Electronic Transport in Mesoscopic Systems, Cambridge University Press, 1997.
[27] S. Braig, K. Flensberg, Phys. Rev. B 68 (2003) 205324.
[28] J. Koch, F. von Oppen, A.V. Andreev, Phys. Rev. B 74 (2006) 205438.
[29] M. Esposito, M. Galperin, Phys. Rev. B 79 (2009) 205303.